Reprinted from JOURNAL OF APPLIED METEOROLOGY, Vol. 9, No. 6, December, 1970, pp. 837–850
American Meteorological Society
Printed in U. S. A.

Aircraft, Spacecraft, Satellite and Radar Observations of Hurricane Gladys, 1968[1]

R. CECIL GENTRY

National Hurricane Research Laboratory, NOAA, Coral Gables, Fla.

TETSUYA T. FUJITA

Dept. of Geophysical Sciences, University of Chicago

AND ROBERT C. SHEETS

National Hurricane Research Laboratory, NOAA, Coral Gables, Fla.

(Manuscript received 26 February 1970, in revised form 21 July 1970)

ABSTRACT

Hurricane Gladys, 17 October 1968, is studied with data collected by Apollo 7 manned spacecraft, ESSA's especially instrumented aircraft, weather search radar, the ATS-III and ESSA 7 satellites, and conventional weather networks. This is the first time data from all of these observing tools have been used to study the structure and dynamics of a hurricane. Techniques used in computing and integrating the various types of data are described and illustrated.

A dominant feature of this immature hurricane was a large cloud which provided a major link between the low- and high-level circulations of the storm. Evidence is presented to suggest this type of cloud and its attendant circulation are features representative of tropical cyclones passing from the tropical storm to the hurricane stage.

1. Introduction

Hurricane Gladys and Apollo 7, the manned spacecraft, by coincidence, were over the Gulf of Mexico at the same time on 17 October 1968. Research aircraft, land based radar, weather satellites, and conventional weather data networks, by plan, were collecting data on hurricane Gladys on this same day. The men in Apollo 7 used Gladys as a target of opportunity and obtained some wonderful pictures of the storm. The combination of these circumstances provided us with a rare opportunity to use data from a number of sources to study the structure and dynamics of a tropical cyclone.

The list of observing tools trained on Gladys is indeed impressive. Two aircraft (one DC-6 and one B-57) from ESSA's Research Flight Facility flew in the hurricane. ESSA's WSR-57 radars at Tampa, Key West and Miami monitored the storm from the outside; ATS-III and ESSA 7 satellites took pictures from above; the conventional surface and upper air weather networks of the United States and neighboring countries collected data on the ambient conditions, and during a 2-min period about 1530 GMT, the Apollo 7 crew took five color pictures of the storm. The research aircraft crews took pictures of the clouds every 2–5 sec, photographs of the radar scopes every sweep, and measurements of wind direction, wind speed, temperature and D values every second.

Hurricanes have been studied in the past with land-based radar data (Wexler, 1947; Kessler and Atlas, 1956; Neuman and Boyd, 1962), with aircraft data (La Seur and Hawkins, 1963; Gentry, 1964, 1967), and with a combination of aircraft and satellite data (Hawkins and Rubsam, 1968a, b; Fett, 1968). It is believed however, that this is the first time so many observational tools were used in a single storm study.

Initially we proposed to determine how best to integrate the output from these various observational tools in a study of a weather phenomenon. In the process of the study we learned several interesting things about an immature hurricane and gained further insight into the mechanism by which the convective and synoptic scales interact to change a tropical storm into a hurricane. In this paper, therefore, we present examples of the various types of data collected and analyzed, show how they complement each other, and discuss the structure and dynamics of the developing storm.

The Apollo 7 pictures of hurricane Gladys (Fig. 1) are dominated by a large circular shaped cloud which was near but to the north of the hurricane center. Analyses showed this to be one of the most interesting features of the storm and to be an essential link in the radial-vertical circulation of mass through the hurricane. We

[1] Portions of this research performed at the University of Chicago have been sponsored by ESSA under Grant NSSL-E-22-41-69.

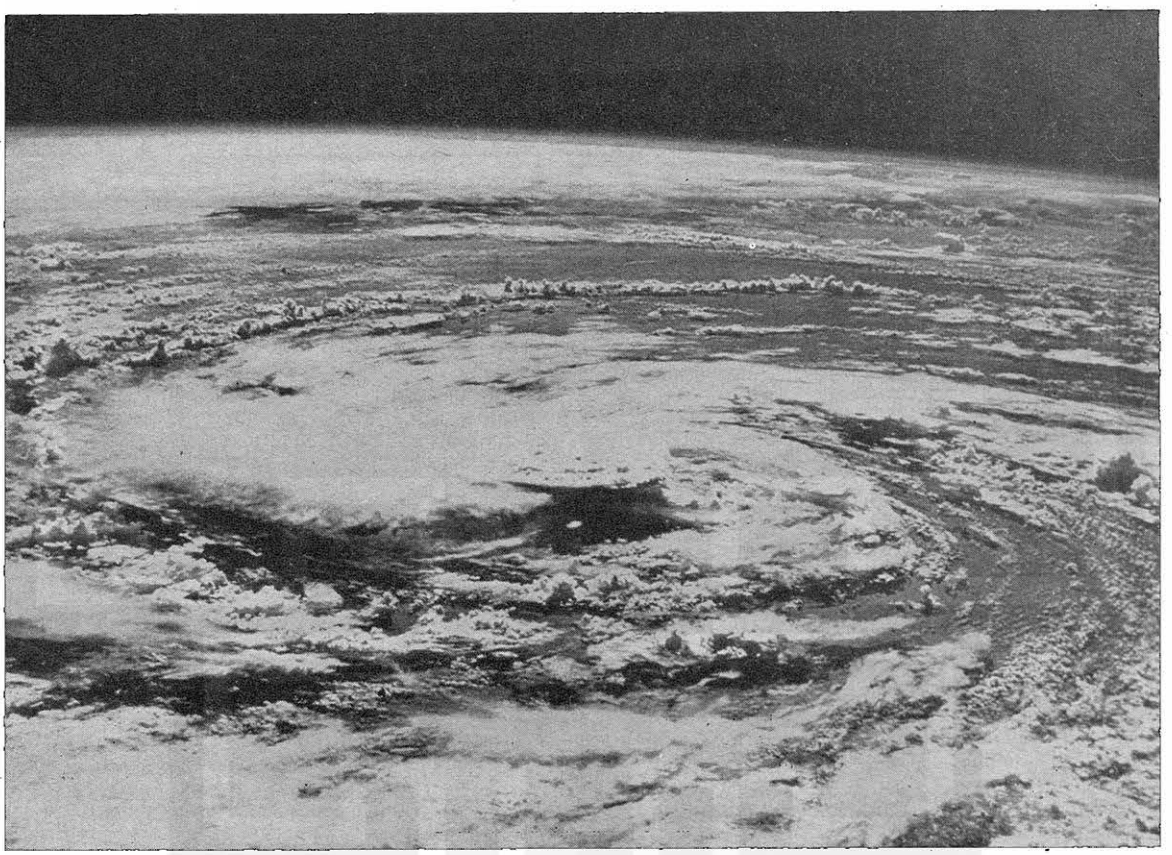

FIG. 1. Apollo 7 view of hurricane Gladys at 1531 GMT 17 October 1968. A saucer-like cloud termed the Circular Exhaust Cloud (CEC) is seen near the picture center some 500 km away. Although the CEC appears to be situated over the hurricane center, later analysis revealed that the center was located at the rear right edge of the CEC. This picture was taken looking southeast toward Havana. The north line through the storm center extends toward the lower left corner of the picture.

called it the Circular Exhaust Cloud (CEC) and we will discuss its formation and evolution in some detail.

2. History of hurricane Gladys

A disturbed weather area formed on the Intertropical Convergence Zone near San Andres in the western Caribbean on 13 October. After drifting slowly north-northwestward, it intensified into tropical storm Gladys on 15 October (Sugg and Herbert, 1969). Gladys reached hurricane intensity before reaching the south coast of Cuba. Although it weakened some while crossing that country, it was near hurricane force when it passed into the Florida Straits area late on 16 October (Fig. 2).

Gladys moved in a general northerly direction during the night of the 16th and during the 17th. By 1500 GMT 17 October, it was centered about 130 n mi west-southwest of Tampa, Fla. Gladys, on this day, was of minimal hurricane intensity (maximum winds measured at 540 m by aircraft were 64 kt), and had a minimum sea level pressure of 986 mb.

Gladys crossed northern Florida during the night of 18 October emerging on the east coast near St. Augustine about daybreak on 19 October. It then moved northeastward over the Atlantic not far from the coastline and eventually became extratropical as it merged with a cold front off the coast of Nova Scotia on 21 October.

3. Analysis of Apollo pictures together with WSR-57 pictures

Since Apollo 7 pictures showing Gladys on 17 October 1968 reveal the fine structure of a weak hurricane presumably well, they have been analyzed by several investigators with varying degrees of precision. Notably, the cover picture of the February 1969 BULLETIN OF THE AMERICAN METEROLOGICAL SOCIETY and the qualitative study by Soules and Nagler (1969) revealed the potential values of detailed study of 70-mm color pictures taken from an earth-orbiting platform.

In order to carry out an accurate photogrammetric analysis of five usable pictures, each negative was enlarged to a size with a principal distance of $f=320$ mm. The print size corresponding to this focal distance is about 9 inches by 9 inches. Fortunately, all are high-oblique pictures, permitting us to compute the picture tilt. After computing the tilt for each picture, Fujita's (1963) method of satellite picture gridding was used to

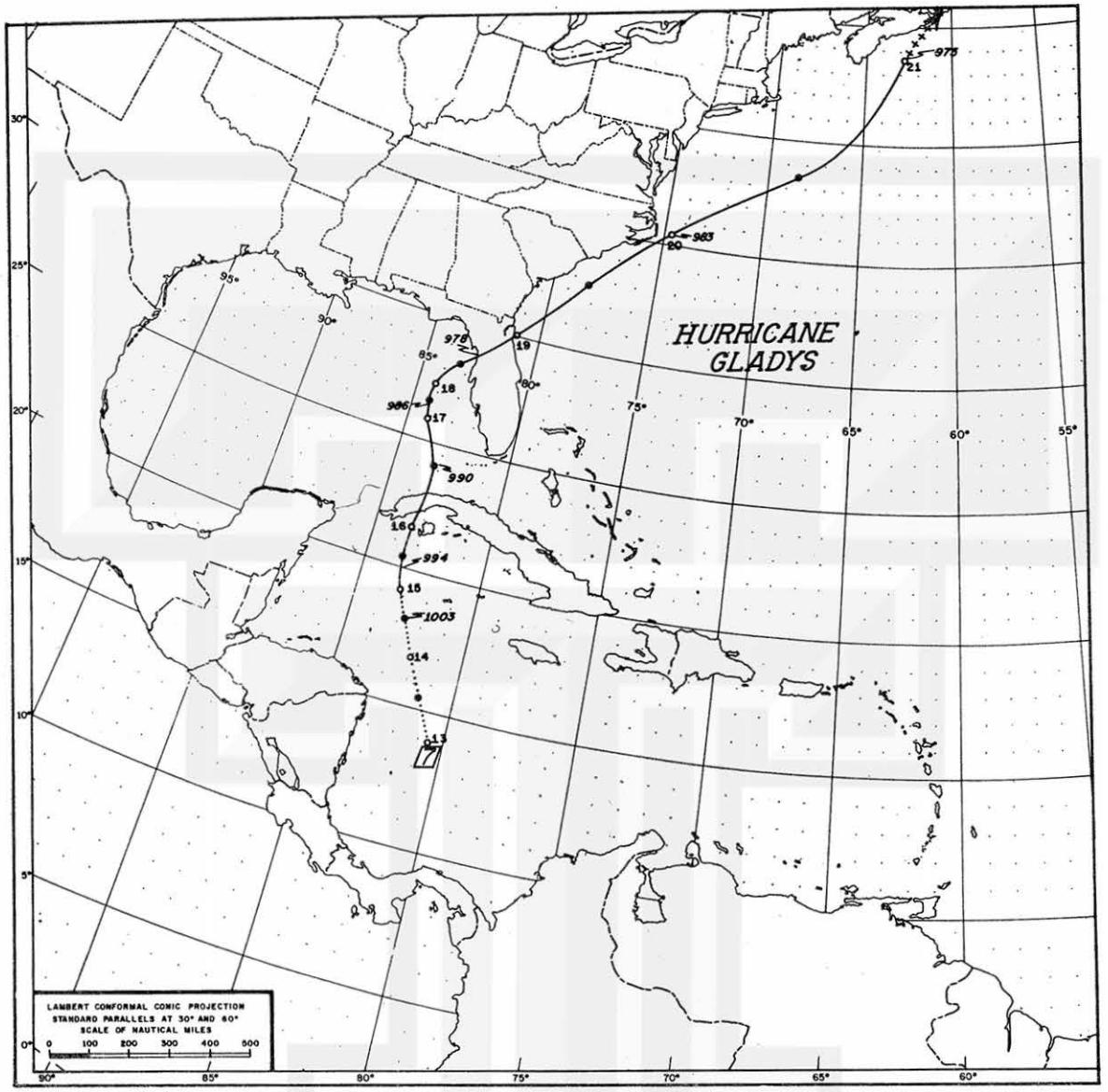

FIG. 2. Track of hurricane Gladys, 13–21 October 1968.

determine photogrammetric quantities as shown in Fig. 3.

Although picture No. 2 included no landmarks whatsoever, approximately 50 cloud shadows plotted on the 1:2,500,000 map from the previous picture were used as if they were small islands floating over the Gulf. The shadow movement between the exposures of pictures 1 and 2, which were about 30 sec apart, is small enough to be neglected. This bridge method developed in this research permitted us to determine photogrammetric quantities from one picture to the next.

To safeguard against amplification of errors in this bridge method, positions of small radar echoes from Tampa and Key West were also used. By doing this, we were able to use small echoes as positions of small precipitating clouds. Thus, we carried on successive photogrammetric analyses to determine the final photogrammetric data in Fig. 3. It should be noted that while the final estimated track of Apollo 7 is quite accurate, the positions of the subpoints at which the pictures were exposed could be up to 1 n mi in error. The distance in geocentric angle between the subpoints of pictures 1 and 5 was ~8°, corresponding to a 2-min travel time by Apollo 7; this resulted in an estimated average picture-taking interval of 30 sec.

The resolution of the picture is so high that even towering cumuli beyond Cuba can clearly be identified. A well-defined cloud band extends from near Cuba to the west of Key West and spirals into the hurricane area. The hurricane center at 1531 shown in Fig. 4, determined from WSR-57 radars at Key West and Tampa, appears near the right edge of the CEC in the

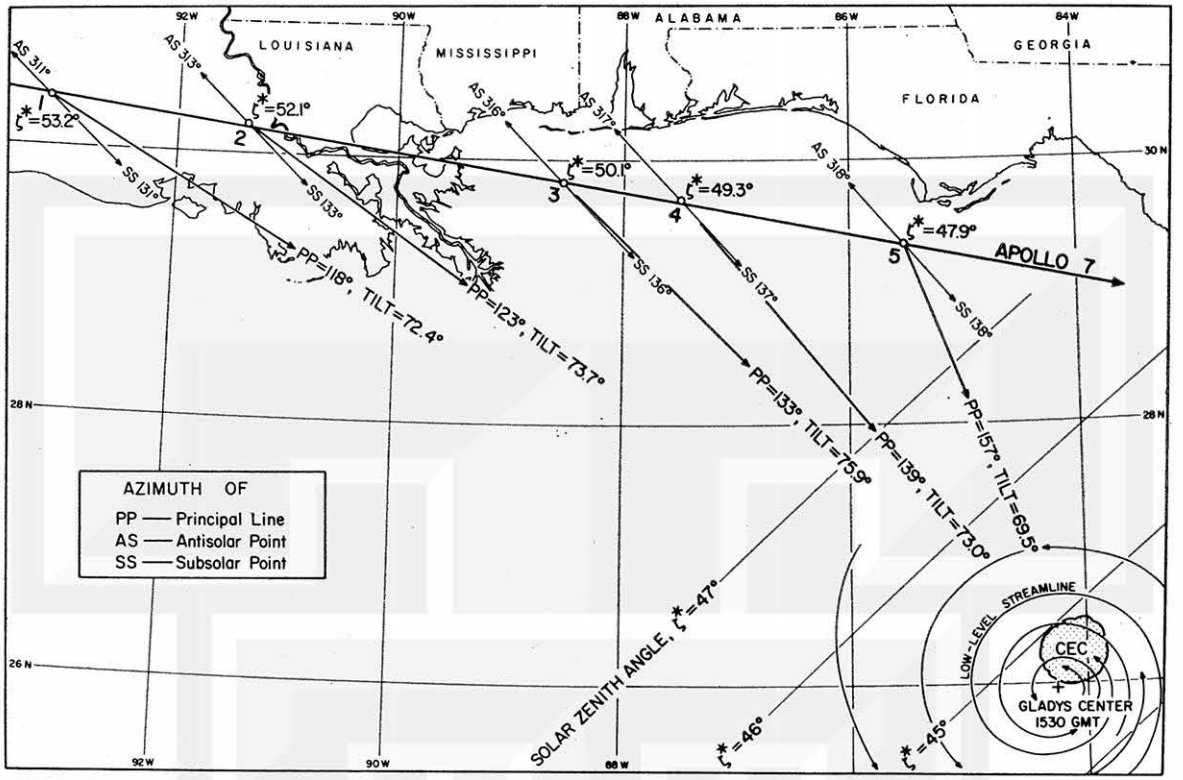

FIG. 3. Apollo 7 track determined from exposure subpoints of pictures 1 through 5 taken between 1530 and 1531 GMT from 99–100 n mi altitude. Sun angle computation indicates that Gladys was illuminated by the sun with solar zenith angle of ~45° from the direction of ~135° azimuth.

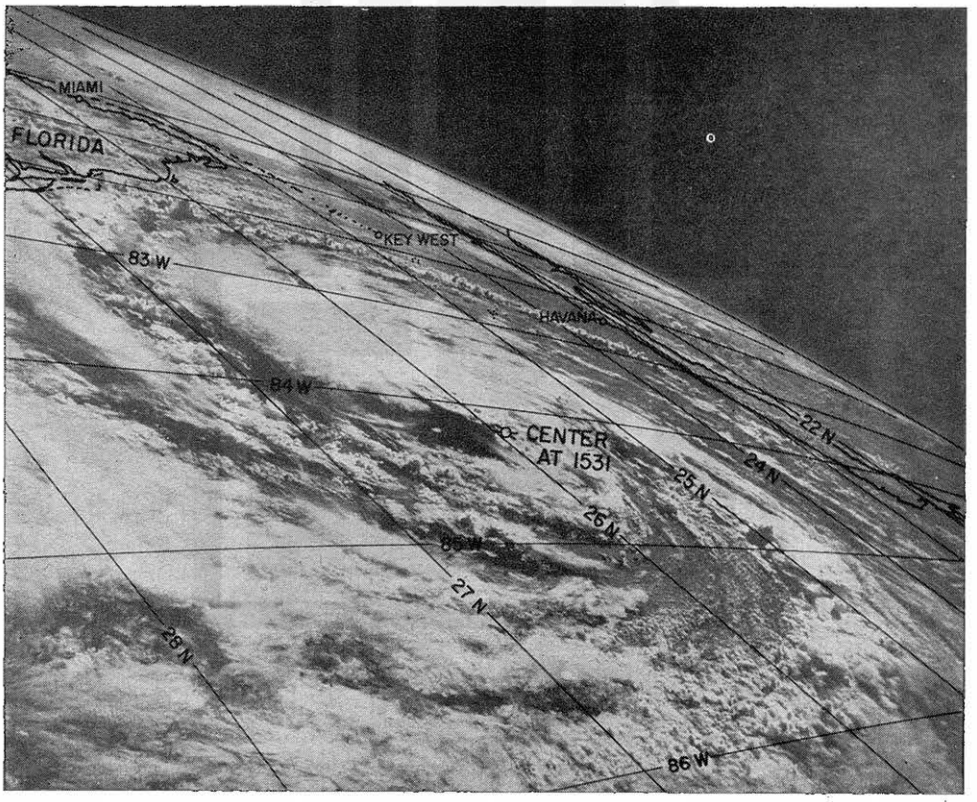

FIG. 4. Apollo 7 picture No. 4 with geographic grids at 1° intervals drawn at sea level. The picture principal line points toward 139° azimuth with a 73.0° tilt. The azimuth of the sun was 137° with the elevation angle 40.7°. Thus, the picture was taken facing toward the sun, resulting in the cloud shadows being cast toward the observer.

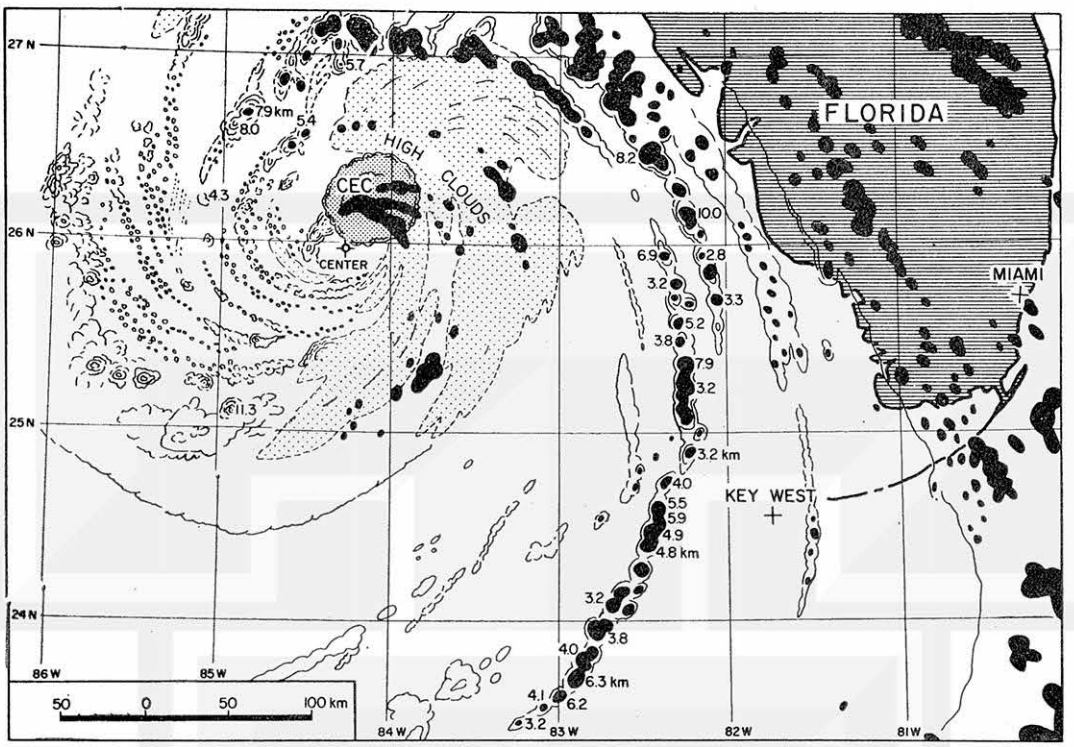

FIG. 5. An example of PPI composite echoes superimposed upon the cloud pattern derived from Apollo 7 pictures. Cloud heights shown by the echoes are in kilometers MSL. The height of the CEC was ~12 km at its rim.

picture. In order to determine the exact relationship between the CEC and the hurricane center, we must project its circular rim down to sea level. Such a projection will shift the cloud position considerably toward the camera. Unfortunately, however, the amount of shift cannot be computed without knowing the height of the CEC above sea level.

Computation of cloud height from aerial or satellite pictures can be performed through standard photogrammetric techniques if stereo-pair pictures are avail-

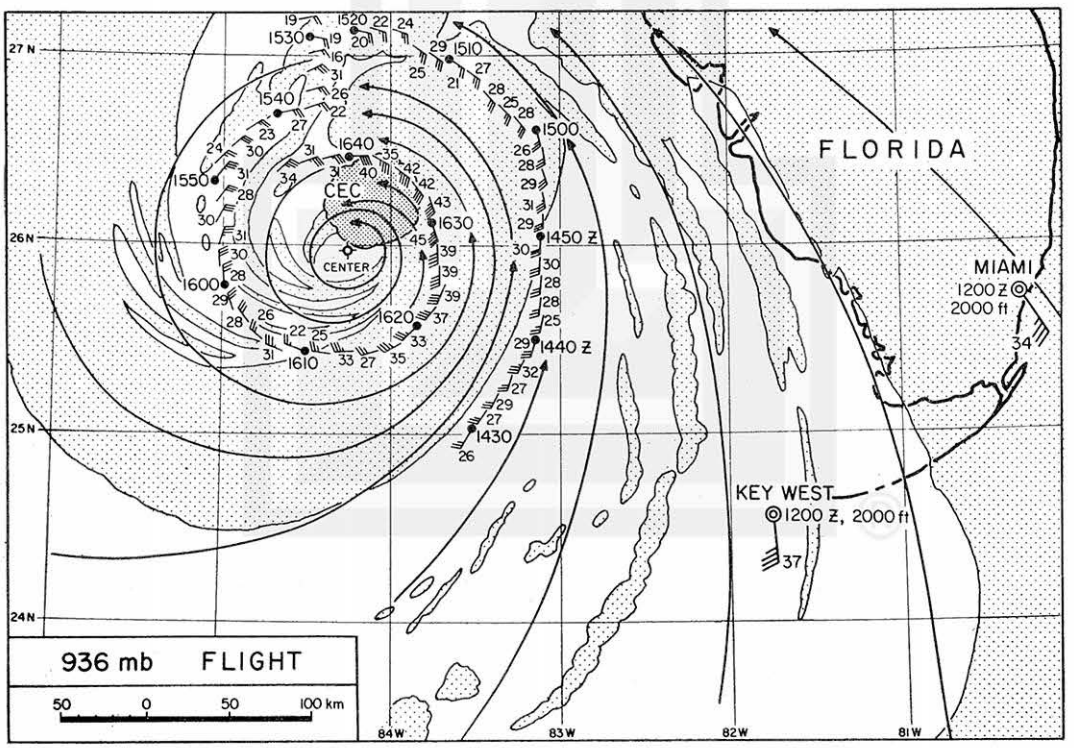

FIG. 6. Streamline analysis of winds recorded near the time of the Apollo 7 pictures on flight at 540 m and superimposed on low-level cloud analysis from Apollo pictures.

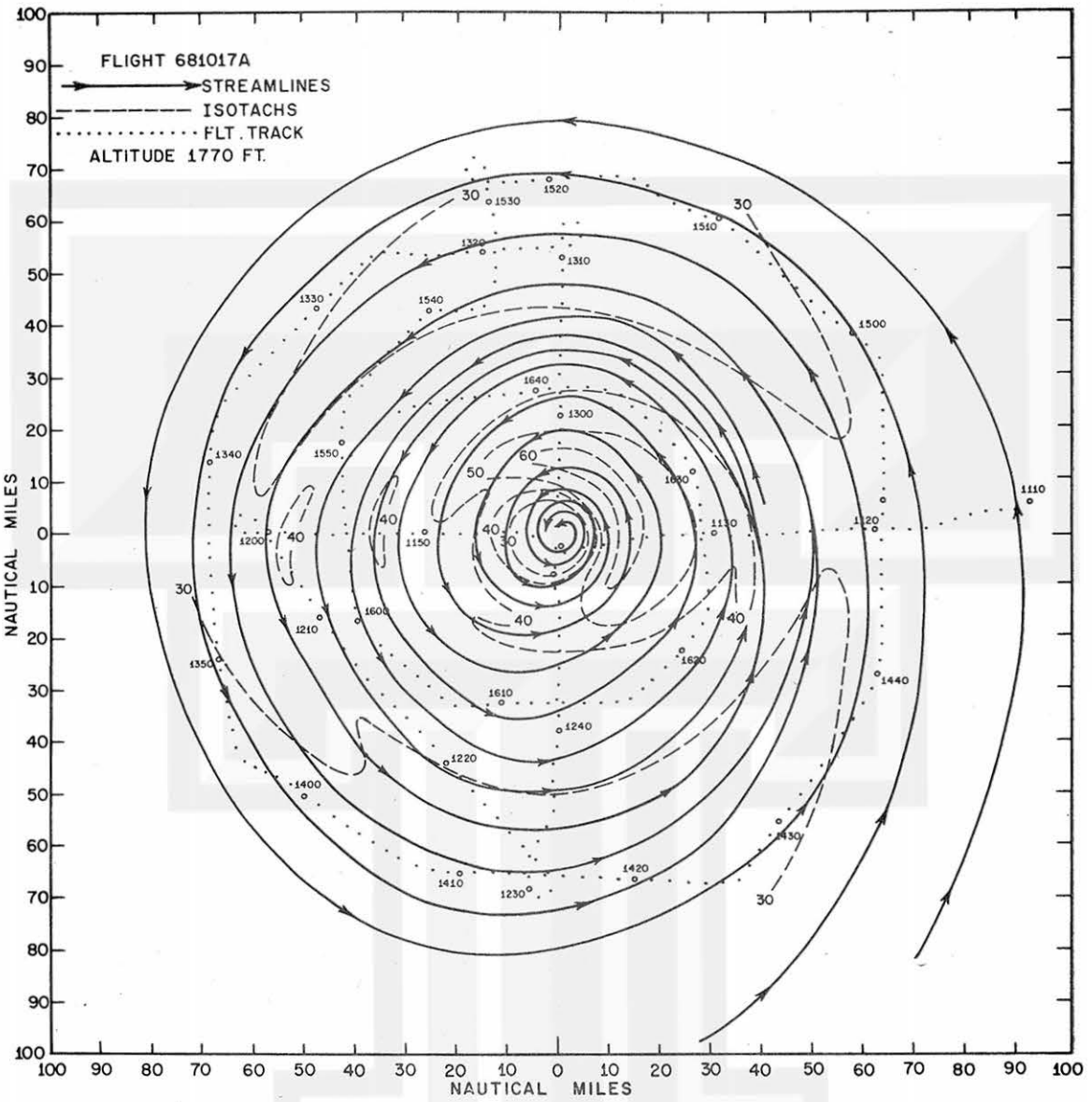

FIG. 7. Streamline and isotach analyses of winds recorded at 540 m on 17 October 1968.

able. An attempt was made to compute cloud heights from pairs numbers 1 and 2, 2 and 3, etc., but it turned out to be unsuccessful. One reason was that the large distance between Apollo and the clouds resulted in height computations by this technique with errors of more than 500 m.

Recently, Fujita (1969) developed a method of computing cloud heights from the length of a vector on the picture connecting a cloud with its shadow. The equations used for the computation permit us to obtain the cloud height as a function of the distance between the cloud and the corresponding shadow, the distance from Apollo to the shadow, the scattering angle, the solar zenith angle at the shadow, and a perspective parameter. This method permits us to compute the cloud height very quickly so long as a cloud and its shadow are identified in a picture. If we measure shadow lengths with 0.2 mm accuracy, the error in cloud height will be about 500 m at the distance of Cuba in Fig. 5. As we approach the lower portion of the picture, 200 m accuracy in the cloud height estimate can be obtained.

An example of a composite prepared from the analyzed Apollo picture and WSR-57 radar pictures taken simultaneously at Key West, Miami and Tampa is presented in Fig. 5. Black areas represent radar echoes which are enclosed by cloud boundaries as determined from Apollo pictures. Heights in kilometers of cloud tops corresponding to these echoes are shown. The areas of clouds extending above the 10-km level (all heights MSL) are stippled.

The height of the CEC at its edge was estimated to be 12 km; its top would be as high as 14 km. Streaks of

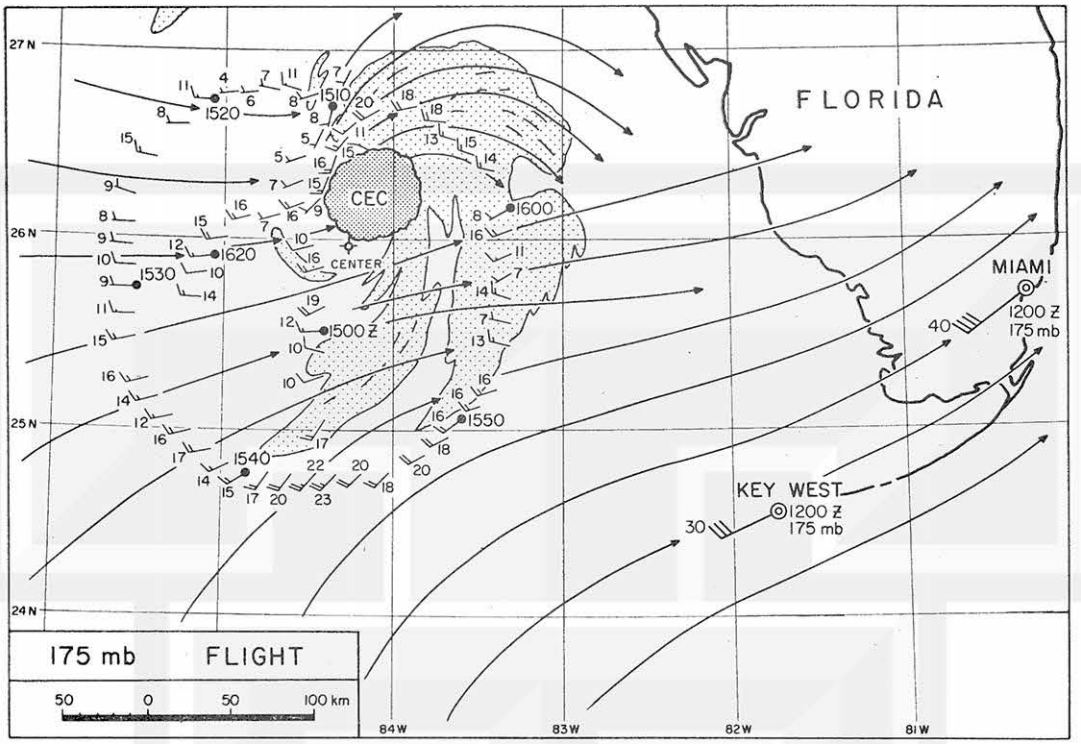

FIG. 8. Streamline analysis of winds at 13,400 m on 17 October superimposed on high-level cloud analysis from Apollo pictures.

high clouds indicate a pattern of outflow stimulated by the expansion of the CEC. A pronounced cloud or echo band extending toward Cuba was made of cellular echoes with the cloud-top height reaching 3–10 km. Most of them, however, had tops at ~5 km. No anvils were seen to originate from these cells. The axes of these clouds appeared to be almost vertical when viewed from the northwest.

The location of the CEC relative to the hurricane center was established after determining its height to be 12 km. It was then learned that the CEC was located over the region of converging echo bands to the north of the hurricane center which is likely to be on a spot on the eyewall where convergence is most significant.

This example of analysis demonstrates that the proper photogrammetric technique permits us to analyze Apollo pictures with high accuracy. Pictures can be used in mapping clouds together with radar echoes. Cloud heights can also be computed from cloud shadows as long as we see them in a picture; and the accuracy of height computation is good enough for research on the fine structure of hurricanes.

4. Aircraft data

a. Cloud structure

The cloud structure as observed from the research aircraft generally reflected the same characteri tics as shown by the Apollo pictures. The cirrus shield was much smaller than that usually associated with more mature or intense hurricanes. Most of the cirrus clouds were over the eastern half of the storm and, even here, were generally broken to occasionally scattered. The low-level flight pattern was confined to within 70 n mi of the storm center (Figs. 6 and 7) except when entering and exiting the storm area. During the circumnavigation of the storm at a radius of 65 n mi, the aircraft was clear of clouds more than half the time. Only occasionally did the low-level clouds observed indicate much vertical development and very few middle level clouds were observed. During the circumnavigation at a radius of 30 n mi and the two radial passes, the only strong convection encountered was in the region of the CEC, north of the storm center. A flight pattern similar to that shown in Fig. 7 was completed at a level of 1950 m (not illustrated) and similar cloud conditions were observed.

The ESSA Research Flight Facility B-57 aircraft flew the pattern illustrated in Fig. 8 over the storm at an altitude near 13,400 m during the period of the Apollo pictures and the low-level flight. The cloud tops approached the aircraft level only in the northeast quadrant, the CEC area, and in a band ~60 n mi south of the storm center. The CEC showed a very distant hard core convective area protruding through the general cirrus outflow level (Fig. 9).

Fig. 9a shows the CEC as observed from the DC-6 aircraft at an altitude of 540 m while Figs. 9b and 9c show the area of the CEC recorded by the forward

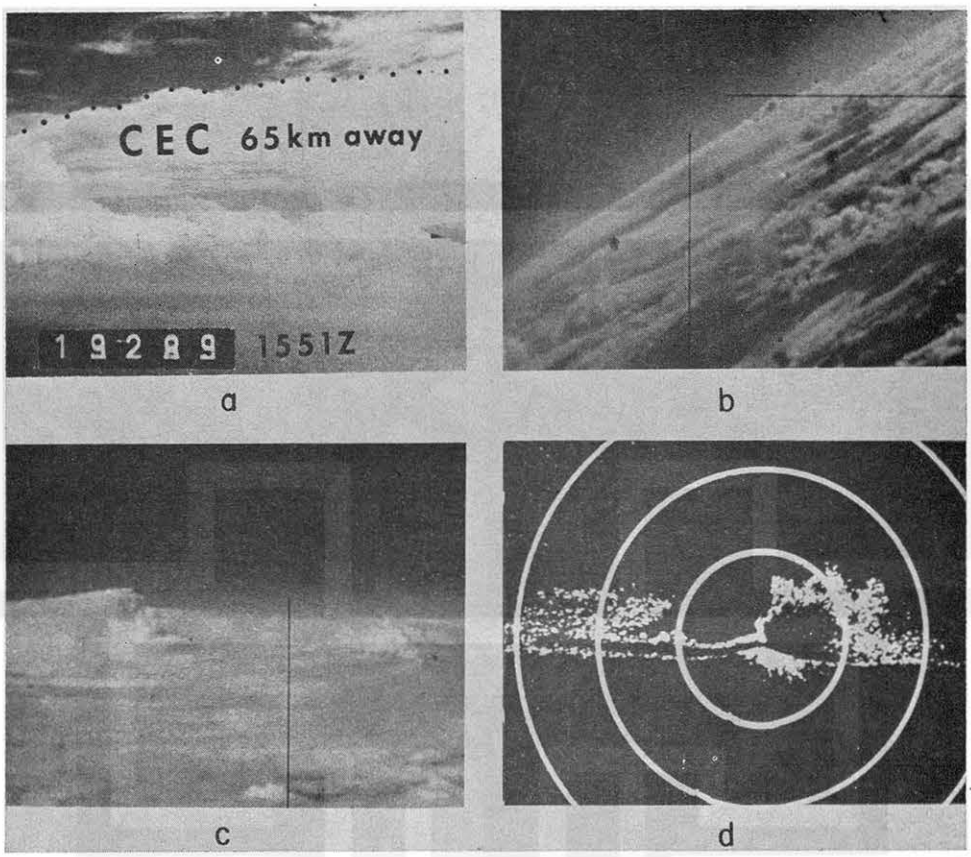

FIG. 9. Composite of four pictures showing the circular exhaust cloud observed from a) DC-6 aircraft at 1551 GMT; b) B-57 aircraft at 1440 GMT; c) B-57 aircraft at 1452 GMT, and d) RDR vertically oriented radar with the CEC centered to the right of the center.

oriented 16-mm camera in the B-57 at 13,400 m. Fig. 9d shows the CEC as observed on the scope of the vertically oriented RDR 3.2-cm radar system in the DC-6 aircraft. The radar system scans a plane normal to the aircraft heading and was being operated in the iso-echo mode. The narrow clear band, slightly below the center of the scope extending both right and left, separates the sea return from the cloud echoes above. The most intense portion of the echo from the CEC is the dark area surrounded by the light area centered just to the right of the center of the scope. The range markers are at 5 n mi intervals and the center of the scope is at the aircraft altitude, 1950 m. The CEC echo then extends to approximately 10,700 m.

b. Low-level wind field

The winds measured during the flight at the 540 m level have been composited with each wind positioned relative to the center of the hurricane. If we assume that the storm was in a steady state during the 3.5 hr needed to collect the data, we can treat these winds as though they were all measured at the same time. We did this in preparing the streamline and isotach analysis of the winds at 540 m shown in Fig. 7. Maximum wind speeds exceeding 60 kt were recorded within 50 n mi of the storm center north and east of the circulation center. The typical spiralling inward flow at this level is illustrated by the streamline analysis.

This analyzed wind field was used in computing the divergence. The winds used were interpolated from the analyses for a 10 n mi grid spacing and smoothed by a 9-point[2] smoothing routine. The divergence field computed from these smoothed winds shows a maximum of convergence of 1.5×10^{-4} sec^{-1} in the vicinity of the CEC (Fig. 10). Convergence was typical of most of the eastern and northern quadrants of the storm but an area of divergence at a radius of 30–40 n mi extended from the western side of the storm around toward the storm center on the south and southeast sides. These latter areas were mostly free of major cloud buildups (Fig. 5).

It is interesting to note the degree of correspondence between the principal cloud features of Gladys and the

[2] The value at each point became the weighted mean of the values at the point and at the eight surrounding grid points with the weights of the latter varying inversely with distance from the point. The value at the point contributed one-fourth of the total. The computations were made using a program prepared by A. Anthes.

vertical motions one may infer from the data in Figs. 7 and 10, even though one may certainly question the accuracy of the divergence values calculated in the described manner. The most notable features of the cloud structure have already been mentioned, that is, the CEC and the relatively low amount of total convective cloudiness for Gladys as compared with the typical hurricane. The coincidence of the area of maximum convergence with the location of the CEC has already been noted. The relatively low amount of total cloudiness may be attributed to the similar relatively small net convergence for the storm area (for example, inside the 60 n mi radius).

The net divergence as computed from circumnavigations at levels below 1070 m at approximately 60 n mi is given for a few tropical cyclones in Table 1. These values were computed from

$$\bar{D}_f=\frac{1}{A_f}\oint V_n dS, \qquad (3.1)$$

where $\bar{D}_f$ is the mean divergence for the area, A_f the area bounded by the circumnavigation portion of the flight (approximately the area inside 60 n mi radius), V_n either the normal or radial component of the wind, and S the curve representing the line of flight. The net divergence in Gladys was a full order of magnitude less than in the other storms. This could account for the relatively low amount of intense convective clouds.

This relatively weak convergence field may also be either the cause or another effect of Gladys being very slow to intensify. Gladys was passing over warm water at the time (McFadden, 1970). The sea surface temperatures were above 28C which is warm enough to supply fuel for an intense hurricane.

c. *Vertically oriented radar cross sections*

Figs. 11a and b show composites of radar echoes from the vertically oriented 3.2-cm radar, profiles of wind speeds relative to the moving storm center, temperatures and relative humidities. All are plotted vs radial distance from the storm center for a north-south oriented pass through the storm. The vertically oriented radar composites were obtained from pictures similar to those shown in Fig. 9d which were taken at 16-sec intervals.

The major echo on the north side of the storm in Fig. 11a is associated with the CEC during its earlier stages. As can be seen, there are few radar echoes on this pass and only the CEC echo exceeds 4009 m (16,000 ft) in height. The other passes through the storm revealed essentially the same structure with only a few echoes outside the area of the CEC with these echoes indicating little vertical development.

A later north-south pass is shown in Fig. 11b and depicts the development and spreading out of the echo

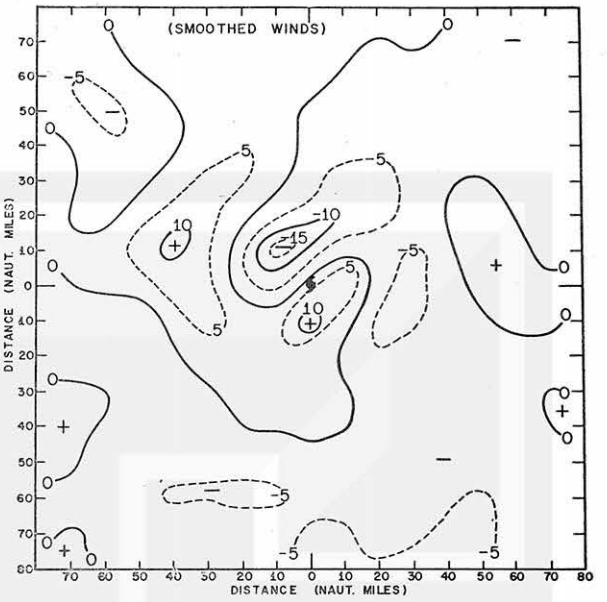

FIG. 10. Divergence field (10^{-5} sec^{-1}) computed from the smoothed aircraft winds illustrated in Fig. 7 at a height of 1770 ft.

associated with the CEC during the day. A series of horizontal radar composites, similar to those in Fig. 5, were constructed using the Tampa and Key West WSR-57 and the airborne radar presentations. These composites (not illustrated) showed the development of the echoes associated with the CEC increasing with time and extending around the northeast and south sides of the eye by 1630 GMT. The major echoes remained in the northeast quadrant, and increased in size and intensity during the day. Many echoes were observed over the eastern and northern portions of the storm with some echoes located as much as 300 n mi from the storm center. At the same time, very few moderate or strong echoes were observed west and southwest of the storm center. This was quite similar to the radar structure observed during the previous day, just after Gladys had passed over Cuba and was in the process of reforming (Sheets, 1969).

TABLE 1. Net divergence in tropical cyclones computed from flight winds.

Name	Date	Flight level (m)	Divergence (10^{-5} sec^{-1})	Approximate maximum winds in storm (kt)
Janice	8 October 1958	480	−11	55
Betsy	1 September 1965	500	−17	80
Betsy	1 September 1965	300	−26	80
Betsy	3 September 1965	1000	−16	125
Betsy	5 September 1965	610	−11	125
Gladys	17 October 1968	540	−1.3	64

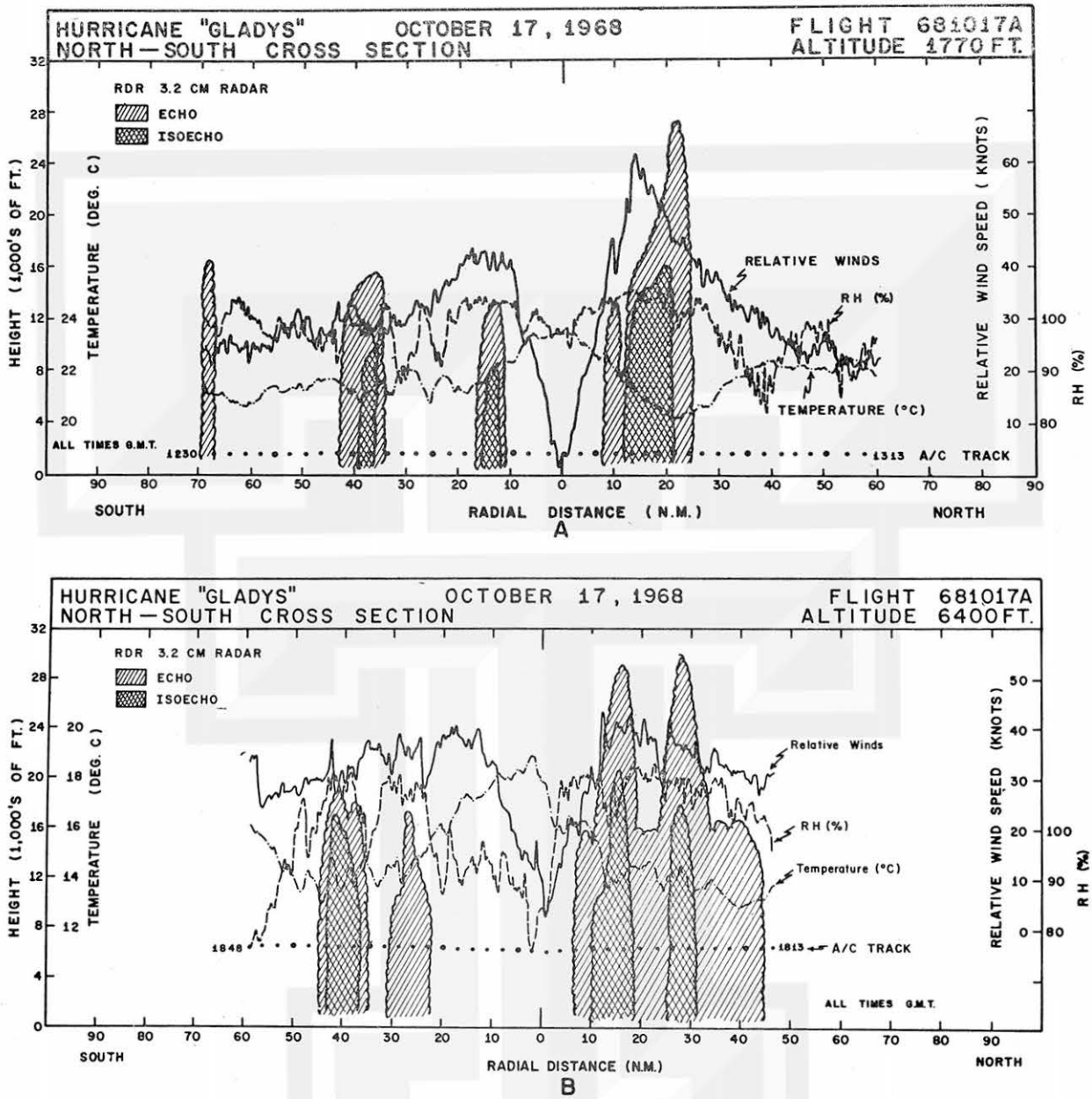

FIG. 11. Cross section of composited radar echoes (from vertically oriented 3.2-cm radar) and profiles of temperature, wind speeds relative to the moving storm center, and the relative humidities for north-south oriented passes through the storm at 1770 ft for 1230–1313 GMT, a., and 6400 ft for 1813–1848 GMT, b. Both sections show echoes from the CEC.

5. A model of the Circular Exhaust Cloud (CEC)

a. The CEC in hurricane Gladys

It is rather unfortunate that no televised satellite pictures of Gladys were available concurrently with Apollo 7 pictures exposed between 1530 and 1531 GMT. ATS-III spin-scan pictures were taken later at 1713, 1927, 1952, 2017 and 2107, as well as ESSA 7 pictures exposed at 1935. Combined analyses of these pictures revealed that the diameter of the CEC increased significantly during the period of the exposures. These diameters as tabulated in Table 2 permit us to estimate the mean divergence inside the CEC at the height of its expanding leading edge if we assume that the cloud edge expanded with the speed of the normal component of the wind. Data are insufficient to fully support this assumption, but results obtained are reasonable. The mean divergence is expressed by

$$\bar{D}_{cec}=\frac{1}{A_{cec}}\oint V_e dS, \tag{4.1}$$

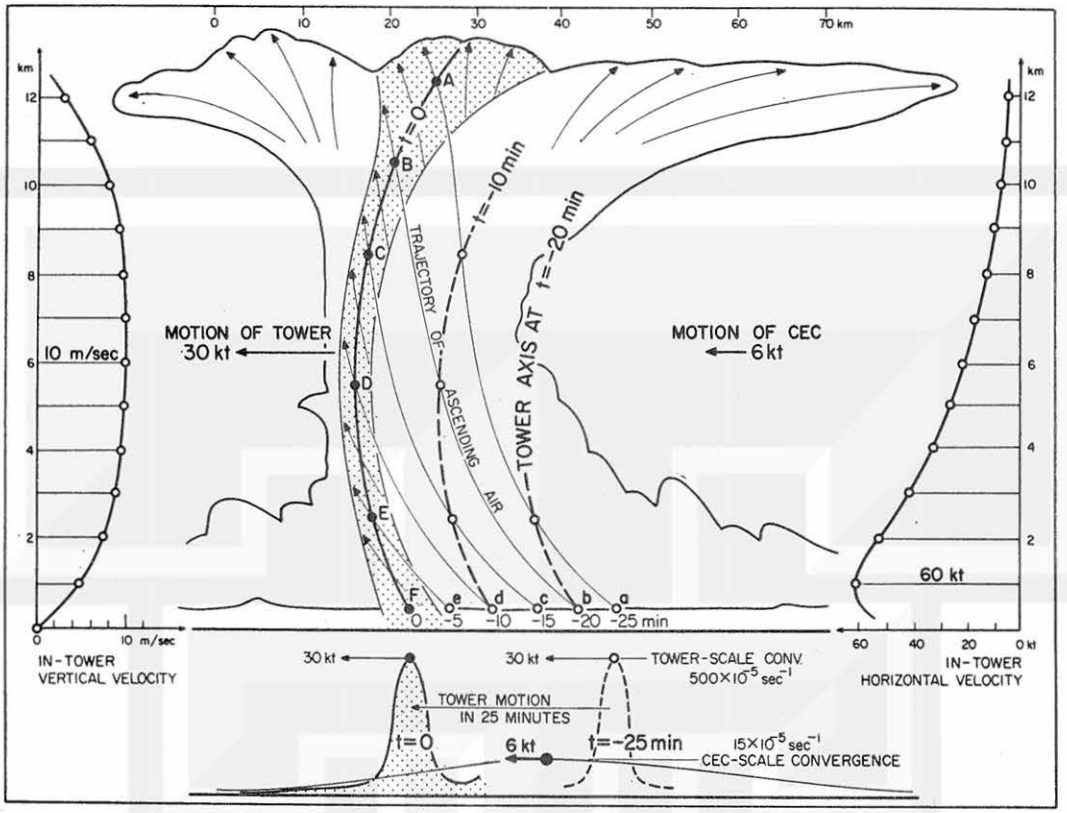

FIG. 12. A model of the circular exhaust cloud based on data for the CEC inside hurricane Gladys of 17 October 1968.

where A_{cec} denotes the horizontal area of the CEC, and V_e the component of expanding velocity normal to the edge segment dS of the CEC. Under the assumption of a circular cloud with constant rate of expansion, we may reduce (4.1) to

$$\tilde{D}_{cec}=\frac{2}{R}\frac{dR}{dt}=\frac{2}{\tilde{R}}\frac{\Delta R}{\Delta t}, \tag{4.2}$$

where R is the radius of the CEC and the tilde denotes the mean value averaged during the period Δt.

The mean divergence thus computed for a 1.7-hr period (1530–1713 GMT) turned out to be 17×10^{-5} sec^{-1}, while that for a 3.1-hr period (1731–2017) was only 5×10^{-5} sec^{-1}. These values indicate that the divergence at the CEC level decreased considerably. But the total expansion rate as defined by

$$\oint V_e dS=A_{cec}\bar{D}_{cec}\approx\pi R^2\bar{D}_{cec}$$

decreased from 2.8 to 2.0 km^2 sec^{-1}. This would mean that the total convective mass transport beneath the CEC remained almost unchanged for ~5 hr after Apollo 7 pictures were taken at 1530.

The displacement of the CEC as a whole is of extreme interest. The CEC center, located some 35 km north-northeast of the hurricane center, rotated in 4 hr by about 100° around the hurricane center which was closely tracked by the land-based radars. The rotation speed of the CEC relative to the storm center was therefore only ~6 kt which is no more than 10% that of the

TABLE 2. Diameter of the CEC measured from various satellite pictures taken on 17 October 1968.

	Time (GMT)					
	1530	1713	1927	1934	1952	2017
Diameter (km)	55	93	110	110	115	120
Determined by	Apollo 7	ATS-III	ATS-III	ESSA 7	ATS-III	ATS-III

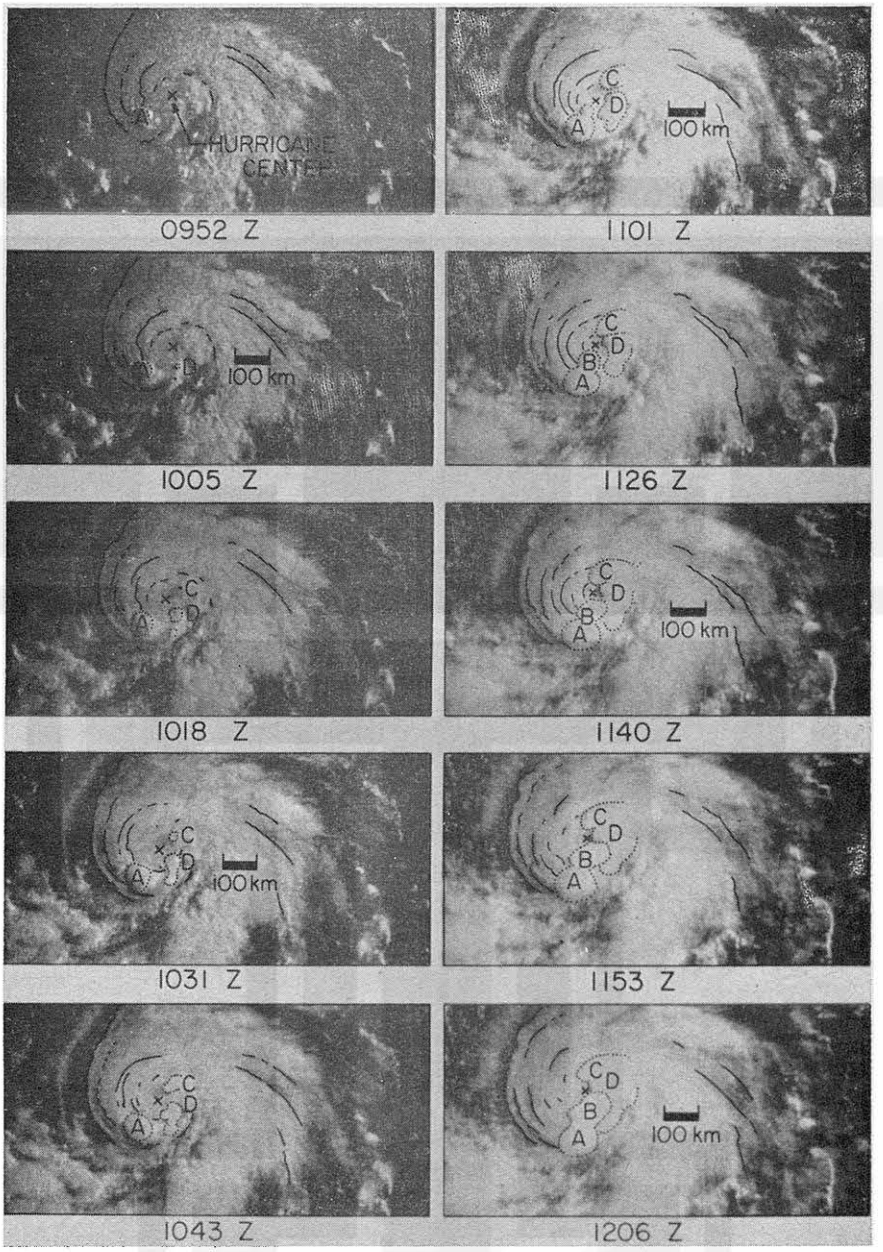

FIG. 13. Time changes in the CEC's seen inside hurricane Debbie of 16 August 1969. Picture sequence was selected from digitized ATS-III pictures produced by NASA for the Hurricane Watch Experiment, 1969.

low-level flow directly beneath the CEC. It is likely that the motion of the CEC corresponds to that of the field of low-level convergence shown in Fig. 10. The maintenance and the motion of such a CEC-scale convergence area is closely related to the asymmetric nature of a hurricane.

While the CEC rotated very slowly around the hurricane center, the WSR-57 Tampa radar indicated that cellular echoes inside the CEC area were moving at the rate of ~30 kt, just about 50% of the low-level wind speed. Evidently, echoes either formed or intensified near the upwind edge of the CEC; meanwhile, continuous dissipation was taking place along the downwind edge.

A schematical cross section of the CEC including a convective tower was constructed in Fig. 12 in which the vertical and the horizontal velocities of the air inside the tower are given to the left and the right, respectively. Step-by-step computations revealed that it would take ~25 min for the inflow air at the cloud base to reach near the cloud top. According to Fujita and Grandoso's (1968) concept of a sliced cloud disc,

the axis of a convective tower and trajectories of parcels occupying various parts of the tower are quite different. For instance, a parcel A near the cloud top must have entered the cloud base 25 min earlier. Its trajectory is shown by a tilted curve connecting a with A. The end points of successive trajectories departing from a through e at the cloud base determine the present shape of the tower axis, A, B, ..., F. It should be noted that the displacement rate of a, b, ..., e is controlled by the propagation of the field of an impulse giving rise to the vertical acceleration of uprising air. In order to account for a gain of some 5 m sec^{-1} vertical velocity within about a 1-km layer above the surface, the impulse should be identified as a convergence field of subcloud convergence of 5 m sec^{-1} (1 km)$^{-1}$=500×10^{-5} sec^{-1}. Despite the significant tilt of the trajectory of ascending air, the tower axis is maintained more or less in an upright position. The figure clearly indicates the major difference between trajectories and the tower axis.

While the maximum convergence beneath each tower is estimated to be ~500×10^{-5} sec^{-1}, the overall convergence beneath the CEC shows a maximum of ~15×10^{-5} sec^{-1}. These values imply that the area of tower-scale convergence is only a few percent of that of CEC-scale conve.gence.

b. The CEC in other hurricanes

The foregoing study suggests that a CEC could be formed where a CEC-scale convergence area is topped by a weak flow at the hurricane outflow level. Most weak hurricanes are characterized by such a structure. In order to find similar CEC's in premature hurricanes, a number of ATS-III pictures were examined. One of the best examples in hurricane Debbie of 16 August 1969 will be discussed.

As shown in Fig. 13, the first indication of a CEC was seen at 0952 GMT on the eyewall southwest of the hurricane center. The cloud identified by A increased its diameter from 50 to 110 km in ~2 hr. The second CEC identified as D appeared at 1005 in a pair. Then they grew and merged. A total of five CEC's were spotted during early morning hours when the low angle of the sun permitted their easy identification.

In most cases the CEC started in the form of isolated point sources such as D at 1005 and C at 1018. These points grew into circular clouds with about a 20-km diameter in less than 15 min.

All CEC's rotated around the hurricane center cyclonically at the rate of 23 kt for A, 20 kt for B, 16 kt for C, and 25 kt for D. The maximum wind speed of Debbie was ~50 kt, indicating that the storm had not reached hurricane intensity yet. It is seen, from these data, that the CEC's rotated at about one-half the tangential wind speed of the parent storm. In the case of Gladys, however, the motion of the CEC was only about 10% of the maximum wind speed around the storm center. Further research on the wind and cloud motion in other storms is required in order to establish their dynamical relationship. Nevertheless, the finding of a number of CEC's in the development stage of Debbie is rather encouraging since we now feel that the CEC could be found in many other hurricanes.

6. Conclusions

Data collected for hurricane Gladys of 17 October 1968, by Apollo 7 manned spacecraft, aircraft of ESSA's Research Flight Facility, ATS-III and ESSA 7 satellites, WSR-57 search radars and conventional weather networks have been integrated in this study of the storm. Description of the various types of data are provided and techniques for utilizing them are explained.

By using data from all the sources, it was practical to deduce features of the three-dimensional mass circulation through the hurricane and to gain new insight concerning the mechanisms by which a hurricane develops. The circular exhaust cloud which dominates the Apollo 7 pictures of the hurricane is a prominent link in this three-dimensional circulation and may be typical of a type of cloud developed in hurricane genesis situations.

REFERENCES

Fett, R. W., 1968: Some unusual aspects concerning the development and structure of Typhoon Billie—July 1967. *Mon. Wea. Rev.*, **96**, 637–648.

Fujita, T., 1963: A technique for precise analysis for satellite data, Vol. 1. Photogrammetry Meteorological Satellite Lab., Rept. 14, ESSA, 106 pp.

——, 1969: A method of computing cloud height from an Apollo picture using cloud shadows. Satellite Mesometeorological Research Project, University of Chicago, Rept. 82 (in press).

——, and H. Grandoso, 1968: Split of a thunderstorm into anticyclonic and cyclonic storms and their motion as determined from numerical model experiments. *J. Atmos. Sci.*, **25**, 416–439.

Gentry, R. C., 1964: A study of hurricane rainbands. National Hurricane Research Project, Rept. 69, Weather Bureau, 85 pp.

——, 1967: Structure of the upper troposphere and lower stratosphere in the vicinity of Hurricane Isbell, 1964. *Papers Meteor. Geophys., Tokyo*, **18**, No. 4, 293–310.

Hawkins, H. K., and D. T. Rubsam, 1968a: Hurricane Hilda, 1964, I. Genesis, as revealed by satellite photographs, conventional and aircraft data. *Mon. Wea. Rev.*, **96**, 428–452.

——, and ——, 1968b: Hurricane Hilda, 1964, II. Structure and budgets of the hurricane on October 1, 1964, *Mon. Wea. Rev.*, **96**, 617–636.

Kessler, E., and D. Atlas, 1956: Radar-synoptic analysis of Hurricane Edna, 1954. Geophys. Res. Paper No. 50, AFCRL, Bedford, Mass., 113 pp.

La Seur, N. E., and H. F. Hawkins, 1963: An analysis of Hurricane Cleo (1958) based on data from research reconnaissance aircraft. *Mon. Wea. Rev.*, **91**, 694–709.

McFadden, J. D., 1970: Airborne investigation of the effects of hurricanes on the thermal structure of the surface layer of the ocean. *Proc. Symp. Investigations and Resources of the Caribbean Sea and Adjacent Regions*, Willemstad, Curacao, 18–23 November 1968 (in press).

Neuman, S., and J. G. Boyd, 1962: Hurricane movement and variable location of high intensity spot in wall cloud radar echo. *Mon. Wea. Rev.*, **90**, 371–374.

Sheets, R. C., 1969: Preliminary analysis of cloud physics data collected in hurricane Gladys (1968). Project Stormfury, Ann. Rept. 1968, Appendix D, 1–11.

Soules, S. D., and K. M. Nagler, 1969: Two tropical storms viewed by Apollo 7. *Bull. Amer. Meteor. Soc.*, **50**, 58–65.

Sugg, A., and P. J. Hebert, 1969: The Atlantic hurricane season of 1968. *Mon. Wea. Rev.*, **97**, 225–239.

Wexler, H., 1947: Structure of hurricanes as determined by radar. *Ann. New York Acad. Sci.*, **48**, Article 8, 821–844.